Early diagnosis of Mycobacterium tuberculosis by detection and quantification of HspX antigen in sputum samples using plasmonic biosensing

Journal:	*ACS Infectious Diseases*
Manuscript ID	Draft
Manuscript Type:	Article
Date Submitted by the Author:	n/a
Complete List of Authors:	Pelaez, Enelia Cristina; ICN2-CSIC-CIBER BBN, Nanobiosensors and Bioanalytical Applications Estévez, Maria Carmen; ICN2-CSIC-CIBER BBN, Nanobiosensors and Bioanalytical Applications Mongui, Alvaro; Corporación CorpoGen, Departamento Biotecnología Molecular Menendez, M.-Carmen; Universidad Autonoma de Madrid, Facultad Medicina. Departamento de Medicina Preventiva, Salud Publica y Microbiología Toro, Carlos; La Paz University Hospital, Department of Microbiology Herrera-Sandoval, Oscar; Centro de Investigación y Desarrollo Tecnológico de la Industria Electro Electrónica y TIC Robledo, Jaime; Corporación para Investigaciones Biológicas, Laboratorio de Micobacterias Garcia, Maria J.; Universidad Autonoma de Madrid, Facultad Medicina. Departamento de Medicina Preventiva, Salud Publica y Microbiología del Portillo, Patricia; Corporación CorpoGen, Departamento Biotecnología Molecular Lechuga, Laura M. ; Institut Català de Nanociència i Nanotecnologia

Early diagnosis of *Mycobacterium tuberculosis* by detection and quantification of HspX antigen in sputum samples using plasmonic biosensing

E.- Cristina Peláez[a,b,c], M.-Carmen Estevez[a], Alvaro Mongui[c], M-Carmen Menéndez[d], Carlos Toro[e], Oscar L. Herrera-Sandoval[b,f], Jaime Robledo[g], Maria J. García[d], Patricia Del Portillo[c], and Laura M. Lechuga[a*]

[a] Nanobiosensors and Bioanalytical Applications Group (NanoB2A), Catalan Institute of Nanoscience and Nanotechnology (ICN2), CSIC, CIBER-BBN and BIST, Campus UAB Bellaterra, 08193 Barcelona, Spain.

[b] Centro de Investigación y Desarrollo Tecnológico de la Industria Electro Electrónica y TIC (CIDEI), Calle 45ª BIS # 19-09 Floor 2, Bogotá DC, Colombia.

[c] Corporación CorpoGen, Departamento Biotecnología Molecular. Carrera 4 # 20-41, Bogotá DC, Colombia.

[d] Departamento de Medicina Preventiva, Salud Publica y Microbiología, Facultad de Medicina, Universidad Autonoma de Madrid, St Arzobispo Morcillo s/n, 28029 Madrid, Spain.

[e] Department of Microbiology. La Paz University Hospital, IdiPaz, St/Paseo de la Castellana 261. 28046 Madrid, Spain.

[f] Research Cluster on Converging Sciences and Technology (NBIC), Universidad Central, Calle 21 #4-40, Bogotá DC, Colombia.

[g] Corporación para Investigaciones Biológicas (CIB), Laboratorio de Micobacterias, Carrera 72A 78B-141, 050034, Medellín, Colombia**.**

[*] *Corresponding author: M.- Carmen Estevez*: mcarmen.estevez@icn2.cat

Abstract

Advances occurred during the last years in the diagnosis of *Mycobacterium tuberculosis* (*Mtb*), the causative agent of tuberculosis infection, have prompted increased survival rates of patients. However, limitations related to the inefficiency of an early detection still remain: some techniques and laboratory methods do not have enough specificity, most instruments are expensive, and require handling by trained staff. In order to contribute to a prompt and effective diagnosis of tuberculosis, we report the development of a portable, user-friendly and low-cost biosensor device for its early detection. By using a label-free miniaturized Surface Plasmon Resonance (SPR) biosensor, we have established a direct immunoassay for the direct detection and quantification of the Heat shock protein X (HspX) of *Mtb,* a well-established biomarker of this pathogen, directly in pre-treated sputum samples. The method relies on highly specific monoclonal antibodies which are previously immobilized on the plasmonic sensor surface. This technology allows the direct detection of the biomarker without amplification steps, showing a Limit of Detection (LOD) of 0.63 ng mL^{-1} and a Limit of Quantification (LOQ) of 2.12 ng mL^{-1}. The direct analysis in pre-treated sputum shows significant differences in the HspX concentration in patients with tuberculosis (with concentration levels in the order of 116-175 ng mL^{-1}) compared with non-tuberculosis infected patients (values below the LOQ of the assay).

Keywords: Tuberculosis diagnosis*;* HspX recombinant protein; SPR Immunosensor; Point-of-Care device; human sputum samples

Tuberculosis (TB) is one of the most impactful infectious diseases with the highest morbidity and mortality in human history.[1,2] According to the World Health Organization (WHO) in 2017, 10.4 million new cases and 1.3 million deaths were attributed to this disease. Moreover, a third of the world's population is calculated to be latently infected, with an asymptomatic and non-transmissible state.[3–5] WHO also estimated that 13 % of tuberculosis patients have HIV[5] and 480.000 cases per year are multidrug-resistant (MDR) owing to inadequate use of antibiotics, poor adherence to anti-TB drugs and to insufficient monitoring of drug resistance.[2,6,7] Around 3 million people who are not diagnosed each year contribute with the high incidence of TB, becoming a source of dissemination of *Mycobacterium tuberculosis* (*Mtb)*.[3] There is a lack of novel detection methods for the diagnosis of TB that can be used in low resource countries, especially in remote populations and that can overcome for instance the low sensitivity of microscopy and the delay in the diagnosis through bacteria culture (around two to six weeks).[2,8] During the infection period, patients without treatment can transmit the bacillus to other people, and therefore a prompt diagnosis could guarantees their survival.[9,10]

Currently, several TB diagnostic methods have been implemented and endorsed by the WHO for the identification of *Mtb,* such as conventional bright field microscopy using Ziehl-Neelsen (ZN) staining,[11] LED-fluorescence microscopy[12] and auramine O staining to identify the presence of Acid-Fast Bacilli (AFB) in sputum smear.[2,13] TB blood tests which evaluate the immunological response to *Mtb* (i.e. Mantoux tuberculin skin test (TST), and Interferon-γ-Release Assays (IGRA))[14,15] are widely applied to diagnose latent TB infection (LTBI). However, TST gives false-positive results in patients who have been vaccinated with Bacillus Calmette-Guérin and both types of tests could give inaccurate responses in patients with immunocompromised conditions as HIV/AIDS.[16] In order to improve the efficiency, specificity and accuracy of the diagnosis, WHO recommended nucleic acid amplification test (NAAT) which uses PCR to amplify and detect mycobacterial rRNA or DNA directly in blood, sputum, and other human biological fluids (i.e. Loop-mediated Isothermal Amplification PCR PURE-TB-LAMP[17,18] and GeneXpert MTB/RIF®.[19] Furthermore, promising biomarkers of *Mtb* such as lipoarabinomannan (LAM),[20,21] ESAT-6,[22] CFP-10,[23] Ag85B,[4] GlcB,[24] and MPT-51[25] found in blood, sputum, cerebrospinal fluid and urine have been studied by ELISA.[26–28] Nevertheless, these techniques are expensive, and still require sophisticated equipment, trained personnel and controlled environments, hindering the TB diagnosis in low-resource settings .[18,29]

For these reasons, WHO recognizes the need for new and more sensitive and specific strategies to improve early TB diagnosis, such as the design of portable Point-of-Care (POC) devices, which stand out as an alternative to the conventional techniques by offering significant advantages as simplicity, portability and affordability. These features can eventually make them accessible to the majority of population, thus helping reduce the global infection rate.[3,30] Several

POC devices based on the detection of *Mtb* biomarkers have been reported. For example, a lateral flow immunochromatography for the detection of LAM in urine is currently commercialized (i.e. Alere Determine™ TB LAM). This biomarker has also been detected in urine using a nanophotonic POC biosensor in a label free configuration[20] or in a planar waveguide based biosensors using fluorescent labeled antibodies.[21] Nevertheless, this lipopolysaccharide is not only found in *Mtb*, but also in other mycobacteria.[31] Other examples are based on the use of Surface Plasmon Resonance (SPR) biosensing for the detection of the CFP-10 antigen in urine,[32,33] Ag85 in sputum[34] and DNA fragments in plasma,[24] the use of a mobile-phone mediated plasmonic ELISA to detect ESAT-6 and CFP-10,[35] or the use of electrochemical devices for the detection of volatile organic compounds (VOC) of *Mtb* (i.e. cyclohexane and benzene derivatives).[36] The use of these biosensors can be inexpensive, simple and fast, but also suffer drawbacks from variable and inconsistent sensitivity (14 – 86 %) and low specificity (47 - 89 %).[37–40]

A critical point in developing a new POC test for TB diagnosis is the selection of the appropriate biomarker to be detected. The heat shock protein HspX (known as α-crystalline homologous or 16 KDa) is secreted along the growth curve of *Mtb* and is a promising *Mtb* biomarker for the early diagnosis of TB[24,26,41] or for the construction of new vaccines .[42,43] Heat shock proteins prevent the aggregation of denatured proteins and facilitate the reassembly by other chaperone proteins. This function is particularly important in *Mtb* because it must withstand extreme environments once it enters the alveolar macrophages, and in turn, forms the granulomas in the lungs.[44] Consequently, HspX stabilizes proteins and cellular structures to survive in this hostile environment, providing a high degree of resistance to the bacteria, escaping the host's innate immune system. This protein is considered as one of the main immunologically active mycobacterial antigen after infection and it is expressed at high levels by bacterial pathogens during adaptation for intracellular survival,[26] which makes it a promising biomarker for the early, rapid and direct detection of *Mtb*.[42] The detection of HspX for active TB has been evaluated mainly by ELISA in human serum,[25,45,46] pleural fluid,[45,47] sputum[45] and cerebrospinal fluid (CSF).[24,45] For latent TB detection has only tested by ELISA in serum.[41,46,48]

To evaluate the potential of the HspX as biomarker for the diagnosis of active tuberculosis, we have implemented a quantitative and label-free SPR based immunoassay for its direct detection in human samples. A direct immunoassay approach using specific monoclonal antibodies previously immobilized on the sensor surface has been fully established, achieving excellent sensitivity and reproducibility. Pre-treated sputum from human samples was directly evaluated, exemplifying the achievement of a rapid and simple test for quantification of the HspX protein. The SPR biosensor has been designed as a portable, user-friendly POC device that requires low

sample volume of pre-treated sputum from TB patients. Our approach could offer a valuable alternative to current available strategies for the early detection and diagnosis of tuberculosis.

Results and Discussion

Cloning, expression and purification of rHspX protein

We have adopted a strategy to express the recombinant HspX protein because we need to obtain a sufficient amount of this antigen in order to perform the optimization of the immunoassays and the quantification of the pre-treated sputums. First, the PCR amplification of *hspX* gene (436 bp) was confirmed by agarose gel electrophoresis as shown in Fig. S2 in SI. The amplified gene was cloned into the vector pET100/D-TOPO and the ligation was evaluated by PCR amplification with the T7 promoter primers of the vector (data not shown). PCR fragments of the expected size (711 bp), corresponding to the *hspX* gene (436 bp) inserted in the TOPO cloning site, were confirmed for correct orientation by a digestion with two restriction enzymes: EcoRI and BgLII (Fig. S3 in SI). Sanger sequencing confirms the correct *rhsp*X gene in two of three selected clones (Fig. S4 in SI). Clone 10 had a mutation in the nucleotide 307 (an A for a G) from start codon and was not used for further analysis.

Transformation of *E. coli* BL21 (DE3) cells were performed in order to express the rHspX by induction with IPTG. According to Taylor *et al*. [43], HspX is expressed in the stationary phase. Therefore, expression of rHspX (diluted 1/10 and 1/100) was analyzed at 4 and 16 h of growth in a western blot using anti-HisG (1:10000) against the N-terminal 6xHis tag of the vector. Fig. S5 in SI, shows the expression of a protein of 16 kDa according to the molecular weight size marker. Expression at 4 h of induction was higher than at 16 h according with the intensity of the bands (Fig. S5 in SI). Likewise, detection with mAb anti-HspX (1:5000) was assessed (data not shown). Solubility tests were carried out to determine in which fractions the highest amount of recombinant protein was present. The rHspX is obtained in both the soluble and the insoluble fraction but a highest concentration is present in the insoluble fraction (Fig. S6 in SI). Protein dimers and trimers are also observed due to bands with a double and triple molecular weight.[49]

The purification of the rHspX was performed by affinity chromatography (using the 6xHis-tagged recombinant protein). The presence of the protein was visualized by SDS-PAGE and western blot. The rHspX was eluted from the retention fraction R1 and R2, as can be seen in Fig. S7 in SI. The protein was dialyzed, lyophilized and diluted in PBS buffer. A stock solution with a final concentration of 84.63 μg mL^{-1} (as determined with the Bradford test) was used for the assay development.

Direct immunoassay development

Ideally, a POC device should allow the detection of analytes in a single step and, if possible, directly in the biological fluid. Thus, a direct assay, based on the immobilization of anti-HspX

as the bioreceptor on the gold sensor chips was selected. A schematic representation of the biofunctionalization strategy, based on the covalent attachment of the antibodies to carboxyl-modified surfaces, and the subsequent direct detection are shown in Fig. 1. Parameters as the composition of the carboxyl SAM and the buffer conditions were evaluated in order to provide an optimal and efficient immobilization. Gold sensor chips were modified using thiol chemistry, preparing a mixed SAM of organic thiols that incorporate a chain of ethylene glycol (EG) in their structure to reduce non-specific adsorption of biological samples.[50] A thiol with a carboxylic end (EG-COOH) was used to attach the antibodies, and another one with a hydroxyl end (EG-OH) to space out the antibodies. Two different ratios 1 mM (3:7 and 7:3) were assessed and the effect of the pH in the immobilization was also evaluated. The immobilization is more efficient at low pHs, mainly at pH 4.0-4.5 as it is summarized in the Fig. S9A in SI. This can be due to the establishment of more favorable electrostatic interactions prior to the coupling between the SAM and the antibody. In this way, the mAb is concentrated slightly on the sensor surface, which increases the reaction yield. All steps of the immobilization of the mAb (20 μg mL^{-1}) for both ratios were monitored *in-situ* in real time by the plasmonic biosensor (see Fig. 2A).

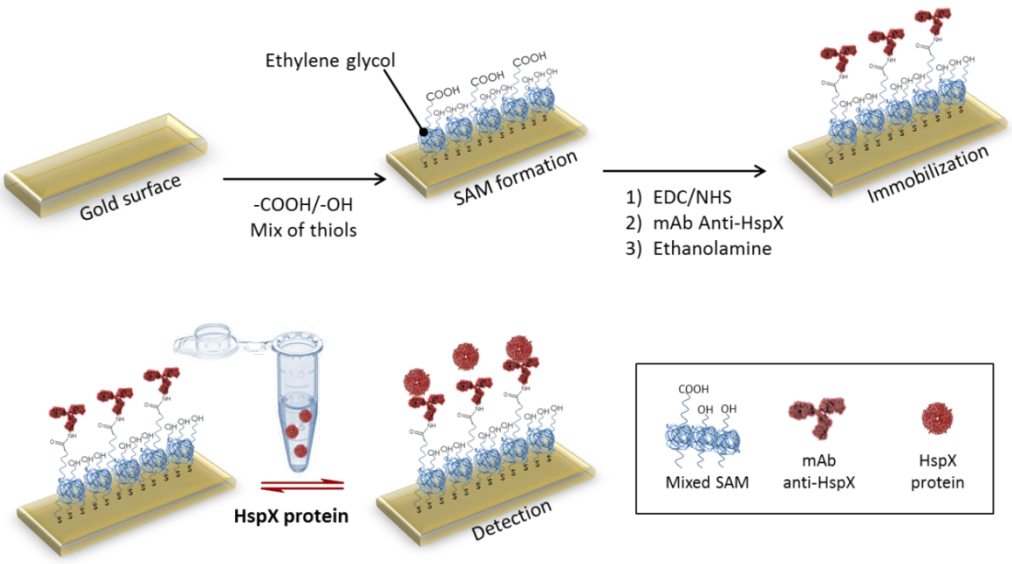

Fig. 1. Scheme of the direct assay employed for the detection of the HspX protein

According to the immobilization values, a pH = 4.0 was selected and the calibration curves based on inter-assays (three calibration curves obtained with three different biofunctionalized chips) for rHspX were obtained for both thiol ratios (see Fig. 2B). The detectability was similar for both ratios (see Table 1), although the maximum signal of immobilization was higher for the COOH:OH ratio of 7:3, which was finally selected. Representative real-time sensorgrams at different rHspX concentrations in PBST are shown in Fig. 2C. In all cases, the average signal-to-noise ratio was very similar ($\Delta\lambda_{SPR}$= 0.0023 ± 0.0009). This low level of noise directly

correlated with a low LOD below 1 ng mL^{-1} (see Table 1). Furthermore, the coefficients of variability (CV) of the inter-assays (especially for the selected combination) confirm the excellent reproducibility and robustness of immunoassays. Finally, the exceptional robustness of the antibody-coated surface robustness was demonstrated through successive regeneration cycles, being possible to get reusable surfaces for at least 33 cycles (see Fig. S9B in SI).

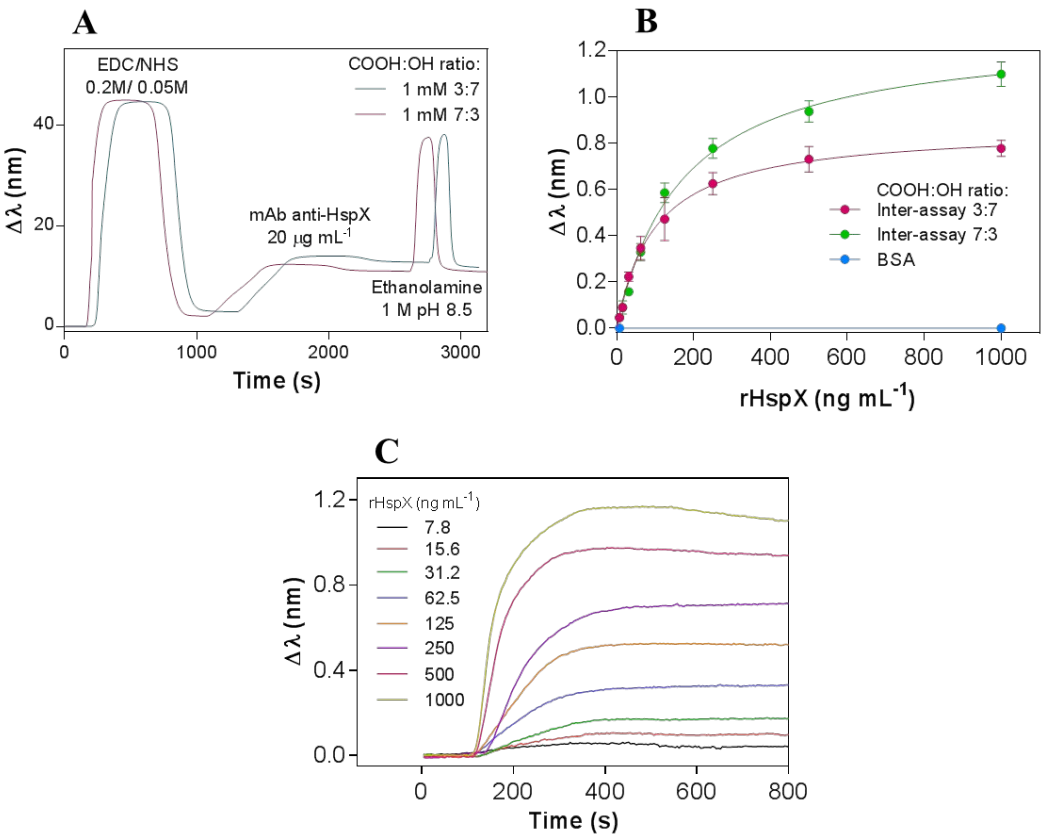

Fig. 2. (A) Real-time SPR sensorgram showing the immobilization steps over 1 mM COOH: OH thiols ratios 3:7 and 7:3 (activation of carboxylic groups, mAb anti-HspX immobilization (20 µg mL^{-1}) in acetate buffer pH 4.0 and blocking with ethanolamine of remaining activated groups). **(B)** Calibration curves of inter-assay in PBST over mAb anti-HspX biofunctionalized (20 µg mL^{-1}, pH 4.0) in COOH:OH ratio 3:7 (pink), 7:3 (green), and BSA as a negative control (blue). **(C)** Real time sensorgrams showing the $\Delta\lambda_{SPR}$ for rHspX over mAb biofunctionalized (20 µg mL^{-1}, pH 4.0) in COOH:OH ratio 7:3 at different rHspX concentrations in PBST.

Sputum matrix effect on rHspX immunoassay

Sputum is a viscous mixture of cellular and biochemical composition of the peripheral airways and the alveolar compartment that appears when there is a chronic inflammatory disease of the respiratory tract such as asthma, chronic bronchitis, tuberculosis or cystic fibrosis. It consists of 95 % water and 5 % solids that vary according to the disease (i.e. carbohydrates, lipids, DNA, filamentous actin, lipids and proteoglycans).[51] This composition might affect the performance of the biosensor (i.e. hindering antibody-antigen interaction or causing non-specific adsorptions). Thus, in order to assess the diagnosis potential of the biosensor, we evaluated the feasibility of

directly measuring sputum samples. As can be observed in the Fig. 3A, untreated sputum coming from non-tuberculous samples (UNTSS) directly injected resulted in a high signal ($\Delta\lambda_{SPR}$= 1.29 ± 0.023) (purple sensorgram), as a result of the non-specific adsorptions of the viscous fluid onto the functionalized sensor chip. However, applying a standard decontamination protocol commonly used with this kind of samples (i.e. PNTSS) resulted in a much lower background (green sensorgram), but not enough to completely eliminate the nonspecific binding. This was finally achieved by further diluting the pre-treated sample in PBST 1:1 (red sensorgram). Under these conditions the interaction of the rHspX with the immobilized antibody was unaffected (see orange and blue sensorgrams for rHspX sample prepared in PBST and PNTSS:PBST 1:1, respectively). The Fig. S9C in the SI shows the real time sensorgrams for different rHspX concentrations prepared in PNTSS (1:1) and the calibration curve obtained with these conditions is graphed in the Fig. 3B and Table 1. Although the signals are slightly lower in diluted pretreated sputum, the detectability parameters are analogous within the linear range (from the LOQ around 2.1 – 2.4 ng mL^{-1} and LOD around 0.6 – 0.7 ng mL^{-1} to saturation signal). CV values, between 5 – 6 % for the inter-assays confirm the excellent reproducibility to enable the direct detection of very low concentrations of HspX in pre-treated sputum samples even after a dilution of 50 %.

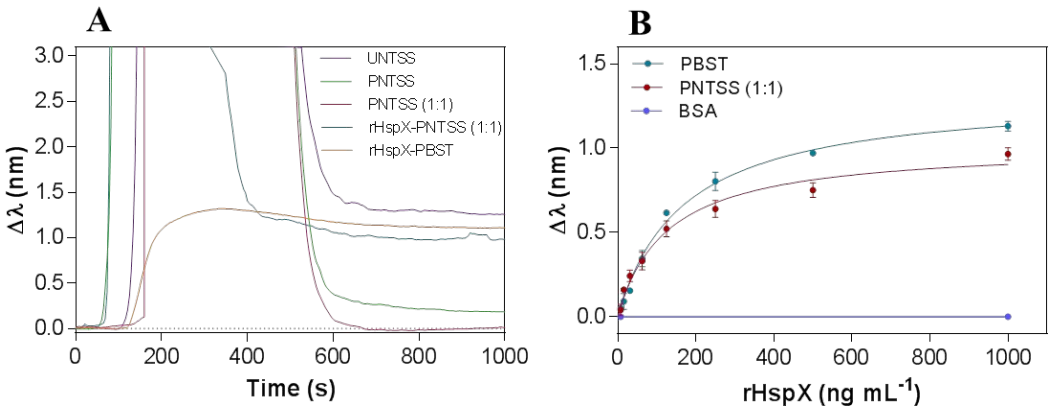

Fig. 3. (A) Matrix effect of untreated non tuberculous sputum (UNTSS, purple line), pre-treated non tuberculous sputum (PNTSS, green line), and PNTSS diluted in PBST 1:1 (red line) over an antibody coated sensor chip (COOH:OH ratio 7:3). No rHspX has been added. Orange and blue line show the rHspX binding (1.0 µg mL^{-1}) in PBST and PTNSS:PBST 1:1 respectively. **(B)** Calibration curves for rHspX protein in PBST and PNTSS:PBST 1:1. Each point represents the mean ± SD of three replicates.

Table 1. Analytical features of direct immunoassays in buffer and pre-treated sputum

COOH:OH Ratio	Protein	Buffer conditions	LOD (ng mL^{-1})[a]		LOQ (ng mL^{-1})[a]	
			Mean ± SD	CV (%)	Mean ± SD	CV (%)
3:7	rHspX	PBST	0.92 ± 0.14	15.2	3.13 ± 0.48	15.3
7:3	rHspX	PBST	0.72 ± 0.04	5.55	2.41 ± 0.13	5.39
7:3	rHspX	PNTSS:PBST (1:1)	0.63 ± 0.03	4.76	2.12 ± 0.11	5.19

[a]: LOD and CV obtained from inter-assays (three calibration curves obtained with three different chips)

Accuracy study with blind samples

The accuracy study was carried out evaluating seven blind samples (B1-B7) of rHspX protein prepared in PNTSS:PBST 1:1 and measured by triplicate. Known concentrations were chosen within and over the working range of the calibration curve. Samples B2, B4 and B6 required additional dilutions (2, 3 and 5-fold respectively) to be within the working range. The results are summarized in Table 2 and as can be observed, recoveries between 97 and 112 % were obtained, which is within the commonly accepted values in conventional immunoassays (i.e. 80-120 %), confirming good levels of accuracy in pre-treated sputum.

Table 2. Accuracy study with blind samples and the SPR immunosensor

Samples	Real concentration (ng mL^{-1})	SPR immunosensor Mean ± SD (ng mL^{-1})[a]	Recovery (%)	CV (%)
B1	70	67.89 ± 1.97	96.99	2.90
B2	200	200.9 ± 3.35	100.4	1.67
B3	50	51.74 ± 2.31	103.5	4.46
B4	300	297.8 ± 7.00	99.27	2.35
B5	10	11.28 ± 0.67	112.8	5.94
B6	500	501.0 ± 10.2	100.2	2.03
B7	20	20.18 ± 1.45	100.9	7.18

[a]: average of three measurements.

Analysis of patient sputum samples

Table 3 shows the level of bacilli seen by microscopy (baciloscopy) as well as the time to positivity and culture results of these samples. We have evaluated 12 pre-treated sputum samples (S1-S12) from five patients, all diagnosed with TB (Table 3A). Up to 22 pre-treated sputum samples from non-tuberculous patients (S13 – S34) were also included as negative controls (Table 3B) as described in the experimental section. All control samples were negative for *Mtb*. NTM (nontuberculous mycobacteria) species were identified in three of them (*M. intracellulare, M. avium and M. celatum* respectively in samples S19, S22 and S26).

Each sample was diluted 1:1 with PBST and measured directly in real-time and replicated twice. Signals were interpolated in the calibration curve with PNTSS (1:1) (see Fig 3B (red curve)). The HspX concentrations for each sample are summarized in Table 3. The median, maximum and minimum values are shown in Fig. 4 for TB and non-TB patients, where significant statistical difference can be observed between them. We found a faint correlation between the concentration of HspX and the level of baciloscopy. The presence of a metabolically variable

population of bacilli in each sample could explain that result. Remarkably, in tuberculous samples previously confirmed by culture methods and Xpert MTB/Rif® but with negative baciloscopy, the detection of the HspX protein was possible, which demonstrates a high sensitivity of our biosensor device (Table 3). Moreover, detection of HspX by SPR biosensor was possible at least one week before positivity of the culture (Table 3A) thus allowing an early diagnosis of the disease. Finally, the SPR procedure developed showed to be *Mtb* specific, due to the absence of cross reactivity with HspX protein of other slow grower mycobacteria.

From our knowledge this is the first work reporting HspX in sputum samples, whose concentration ranges between 116 to 175 ng mL^{-1}. These values are lower than those reported in cerebrospinal fluid, where HspX has been detected in concentrations up to 18 µg mL^{-1}.[24]

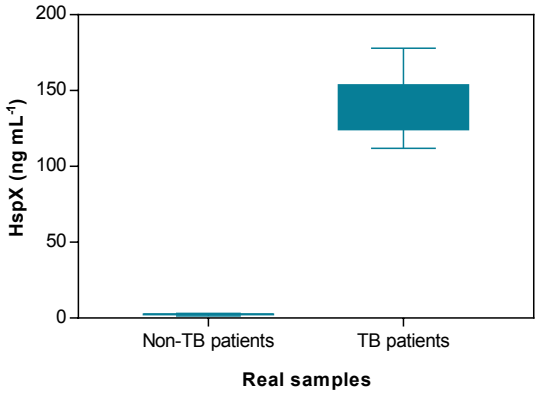

Figure 4. Levels of HspX protein concentration of pre-treated sputum samples from tuberculous (TB) patients (n=12) and non-TB patients (n=22). Median, maximum and minimum values are shown.

Conclusions

We have designed and developed a complete strategy for the direct and label-free detection of HspX TB antigen employing a SPR biosensor. Our approach provides a reliable, reproducible and sensitive detection of the protein in sputum samples, it requires low volume of sputum samples and has a short turnaround time (only 35 - 40 min considering pre-treatment of sputum and analysis) which makes it especially attractive for an early diagnosis of TB. An effective protocol for the expression and purification of HspX protein has been set up, obtaining a high expression yield in just four hours. This has allowed obtaining a sufficient amount of protein to perform the entire assay development and optimization. The biofunctionalization strategy based on EG thiols provides a simple and robust sensing layer for biofunctionalization although the pre-treatment of sputum is still needed to obtain a reliable analysis of the biomarker. Applying this pre-treatment facilitates however its direct analysis, without the need of using any additional amplification step, reaching a LOD of 0.63 ng mL^{-1} and a working range between 2.1 and approximately 125 ng mL^{-1}. The biosensor based assay shows an excellent accuracy, as

demonstrated with recovery values close to 100 % when blind samples were analyzed. Finally, the analysis of real sputum samples from TB patients confirmed the diagnostic potential of the biosensor tool, being possible to observe significant statistical differences between TB and non-TB samples. Concentrations of HspX protein up to 175 ng mL^{-1} were detected. From our knowledge, this is the first reported concentration values reported for this biomarker in sputum. Although more data might be needed to confirm the sensitivity and specificity that we have seeing of this biomarker for early detection, our results pave the way towards the implementation of such analysis in a portable, miniaturized POC platform as a fast and user-friendly tool for clinical diagnosis practice, which could eventually be used during the check-up in primary healthcare units.

Table 3. Clinical sputum samples analysis

(A)	Sputum sample	Patient	BL[a]	[HspX] (µg mL^{-1}) Mean ± SD	CV (%)	TTP (days)	Culture
Tuberculous patients	S1	1	4	146.6 ± 34.1	23.26	7	+
	S2	1	4	123.2 ± 10.1	8.20	10	+
	S3	1	2	147.0 ± 4.4	2.99	ND	ND
	S4	1	4	162.9 ± 4.3	2.63	ND	ND
	S5	2	0	140.0 ± 15.3	10.91	18	+
	S6	2	1	134.0 ± 29.1	21.74	10	+
	S7	2	0	116.3 ± 1.8	1.61	16	+
	S8	2	0	129.1 ± 24.4	18.92	12	+
	S9	3	1	142.4 ± 0.4	0.30	14	+
	S10	4	2	175.0 ± 4.0	2.30	14	+
	S11	5	4	141.5 ± 1.7	1.21	7	+
	S12	5	4	143.6 ± 1.3	0.90	7	+
(B)	**Sputum sample**	**Patient**	**BL[a]**	**[HspX] (µg mL^{-1}) Mean ± SD**	**CV (%)**	**TTP (days)**	**Culture**
Non-Tuberculous patients	S13	7	0	2.13 ± 0.18	8.39	NA	NA
	S14	8	0	1.88 ± 0.18	9.50	NA	NA
	S15	9	0	1.62 ± 0.17	10.9	NA	NA
	S16	10	0	2.51 ± 0.36	14.2	NA	NA
	S17	11	0	2.38 ± 0.18	7.51	NA	NA
	S18	12	0	1.88 ± 0.17	9.50	NA	NA
	S19	13	0	2.64 ± 0.18	6.80	NA	NA
	S20	14	0	2.50 ± 0.34	13.6	NA	NA
	S21	15	0	2.56 ± 0.07	2.80	NA	NA
	S22	16	0	2.69 ± 0.11	4.01	NA	NA
	S23	17	0	2.67 ± 0.09	3.35	NA	NA
	S24	18	0	2.70 ± 0.09	3.32	NA	NA
	S25	19	0	1.95 ± 0.29	14.6	NA	NA
	S26	20	0	2.42 ± 0.23	9.62	NA	NA
	S27	21	0	2.41 ± 0.14	5.95	NA	NA
	S28	22	0	2.67 ± 0.09	3.35	NA	NA
	S29	23	0	2.65 ± 0.20	7.45	NA	NA
	S30	24	0	2.67 ± 0.13	4.70	NA	NA
	S31	25	0	2.84 ± 0.25	8.86	NA	NA
	S32	26	0	1.86 ± 0.12	6.70	NA	NA

S33	27	0	2.41 ± 0.21	8.90	NA	NA
S34	28	0	2.55 ± 0.05	2.11	NA	NA

[a]: BL: Baciloscopy levels: 0 = none; 1= paucibacilary to 4= multibacilary); TTP: time to positivity of the culture; ND: no data; NA: not applicable

Experimental section

Study patients and sputum sampling

A total of 12 pre-treated tuberculous sputum samples (PTSS, S1-S12) from five patients were included in the study, and 22 pre-treated non-tuberculous sputum samples (PNTSS) from 22 patients (S13-S34) were evaluated and employed during the optimization of the immunoassays. In addition, two samples of untreated non-tuberculous sputum sample (UNTSS) were used as a control of sputum matrix. All samples (pre-treated or untreated samples) were collected in sterile containers for diagnostic purposes by the Service of Clinical Microbiology from La Paz University Hospital Madrid (Spain). The local Ethics Committee Hospital La Paz approved the study protocol. Standard diagnostic procedures were performed to test the presence of *Mtb* bacilli in the samples, including fluorescent acid-fast staining and growth in liquid medium BACTEC MGIT 960 (Becton Dickinson) as well as in solid medium Löwenstein-Jensen. The GenoType Mycobacterium CM (Bruker) or Xpert MTB/Rif® (Cepheid) were used for *Mtb* confirmation.

Pretreatment for decontamination of samples has followed standard procedures. In brief, a mixture of N-acetyl-L-cysteine, sodium citrate and NaOH was added to the sample until complete dilution and then it was neutralized with PBS buffer pH 6.8 (BBL™ MycoPrep™, BD). Finally, samples were centrifuged at 4 ºC, 3000 g for 15 min. The supernatant was discarded in a bottle with sodium hypochlorite (5 g L^{-1}) leaving a sediment of 500 µL. These pretreated samples were stored at -20 ºC until analysis. Aliquots of these pre-treated samples (PTSS) were placed in Eppendorf tubes containing a guanidine chloride buffer (preservative agent that halts the bacterial metabolism) and glass beads. The untreated non-tuberculous sample (UNTSS) was placed only in the guanidine chloride buffer. In order to lyse the bacteria, the aliquots were subjected to 7 pulses of lysis with a speed of 5.0 m s^{-1} during 60 s, in a fastprep-24, and maintaining the samples in ice between pulses. The supernatant was collected by centrifugation at 4 ºC, 12000 rpm during 5 min and stored at -70 ºC until analysis.[52] The obtained lysate supernatants were evaluated with the SPR biosensor.

Bacterial strains and growth conditions

Recombinant protein (rHspX) was produced in bacterial expression systems at Corporación Corpogen (Bogotá, Colombia). Reference DNA H37Rv of *Mtb* was obtained from Corporación para Investigaciones Biológicas (CIB) (Medellín, Colombia). Conservation strain *E. coli* TOP10 and competent strain *E. coli* BL21 (DE3) were acquired from Thermo Fisher (Massachusetts,

USA). Strains were grown in Luria-Bertani broth (LB) and LB agar plates, ampicillin (100 μg mL^{-1}) was added to the media when required.

Cloning, expression and purification of rHspX

Amplification of the encoding *hspX* gene, 436 base pairs (pb) was carried out by PCR using as template the genomic DNA of *Mtb* H37Rv. The following upstream and downstream primers were used for the PCR: 5'-CAC CGC CAC CAC CCT TCC-3' and 5'-TCA GTT GGT GGA CCG GAT CT-3'. The amplification product was visualized by electrophoresis in agarose gel stained with SYBR Green. The PCR product was purified and ligated into the vector pET100/D-TOPO (5760 bp) (Thermo Fisher Scientific, Massachusetts, USA) and cells of *E. coli* TOP10 were transformed. The plasmid map of pET100/D-TOPO vector with the gene *hsp*X is depicted in the Fig. S1 in SI. The clone containing the *hsp*X gene was verified by sequence (Macrogen, Inc, Korea). For the expression of the rHspX, the plasmid pET100-hspX was transformed in *E. coli* BL21 (DE3) (Invitrogen, Carlsbad, CA, USA). The transformed *E. coli* was plated on LB media containing ampicillin (100 μg mL^{-1}). The recombinant clone was cultured in liquid media (LB) supplemented with ampicillin and the expression of the protein was induced with isopropyl-β-D-1-thiogalactopyranoside solution (IPTG, 0.5 mM), incubated at 37ºC, 200 rpm for 4 and 16 h [27,43,45]. Cells were broken by FastPrep (Thermo Scientific, MA, USA), (3 cycles at a speed of 5.0 m s^{-1}, for 40 s, leaving samples on ice for 5 min between each cycle).

The soluble and insoluble fractions of rHspX were analyzed by polyacrylamide gel electrophoresis SDS-PAGE 14 % and by western blot. The recombinant protein was detected using anti-HisG (anti-histidine) 1:10000 f or 1 h and with the monoclonal antibody anti-HspX (Abcam, Cambridge, UK) 1:5000 for 2 h. Anti-mouse IgG 1:5000 was used as a secondary antibody. The immunorecognition was detected by the peroxidase enzyme kit.[53] Subsequently, protein was purified by Ni^{2+} chromatography of 50 % Ni-NTA purification system following the manufacturer instructions. Both, the non-retained fraction and the retained fraction were evaluated by electrophoresis and western blot. Finally, the culture of *E. coli* BL21 (DE3) was scaled to 1.5 L, purified and dialyzed by Float-A-lyzer G2 Dialysis device MWCO: 8-10 KDa (Spectrumlabs, FL, USA) in Milli-Q water, then, lyophilized at 0.5 mbar and -51.7 ºC (Telstar Cryodos, UK). The final concentration of HspX protein was quantified by Bradford's reagent (Bio-Rad, UK).

SPR biosensor device

The rHspX detection assays were developed with a homemade compact SPR device. A schematic representation of the sensing principle and a picture of the plasmonic biosensor platform are shown in Fig. S8A in the SI. The optical components of the SPR biosensor and the fluidic channel to keep running fluid continuously over the gold sensor chip (glass surface coated with Ti 1 nm/Au 49 nm) have been previously described.[54] The resonance spectra of the

sensor chips shows a minimum in the reflection at λ_{SPR} (675 nm), which is monitored in real-time *via* polynomial fit using custom designed readout software (see Fig. S8B in SI). Chemical interactions occurring at the gold sensor surface (i.e. biointeraction events) generate variations of the RI which correlates with wavelength displacements of the minimum ($\Delta\lambda_{SPR}$). Therefore, λ_{SPR} is directly related to mass changes resulting from binding events (leading to higher RI and shifts to higher wavelengths) or desorptions (leading to lower RI and shifts to lower wavelengths) occurring on the surface (Fig. S8C in SI).

Surface functionalization

Gold sensor chips were cleaned by heating and sonication for 1 min each step with acetone, ethanol and Milli-Q water. Then, the chips were dried with N_2 stream and dipped in a freshly prepared piranha solution (H_2SO_4/H_2O_2, 7:3) for 1 min. Finally, they were rinsed with Milli-Q water, ethanol and dried with N_2 stream. A mixed self-assembled monolayer (SAM) was formed on the gold sensor surface with a solution of thiols HS-C11-$(EG)_6$-O-CH_2-COOH (EG-COOH) and HS-C_{11}-$(EG)_4$-OH (EG-OH) (EG-COOH:EG-OH,1 mM). The sensor chips were immersed in the thiol solution and heated at 40 ºC for 10 min. Then, they were incubated overnight at room temperature. The sensor chips were placed in the optical platform and closed with the microfluidic cell for biofunctionalization. The antibody immobilization was performed under a continuous flow of Milli-Q water. The carboxylic groups of the generated SAM were first activated as carbodiimide esters by flowing a mixed solution of EDC/NHS (0.2 M /0.05 M) in MES buffer for 30 min at 20 µL min^{-1}. Subsequently, an anti-HspX monoclonal antibody (mAb) solution (20 µg mL^{-1}) was injected at 15 µL min^{-1}. The remaining unreacted groups were then deactivated with an aqueous solution of ethanolamine (1 M pH 8.5) for 2 min at 30 µL min^{-1}. Finally, antibody-biofunctionalized sensor chips were kept under a continuous flow of PBS or PBST buffer at 30 µL min^{-1}.

SPR direct immunoassay performance

A calibration curve of the detection of the rHspX was obtained after evaluating different protein concentrations (between 7.8 and 1000 ng mL^{-1}) from a stock solution of rHspX (84.6 µg mL^{-1}). Triplicate analysis was carried out for each concentration. Each standard sample was injected randomly over the antibody coated sensor surface at a flow rate of 30 µL min^{-1}. A regeneration process to dissociate the antigen-antibody interaction was achieved by injecting 3 mM NaOH at 35 µL min^{-1} for 120 s. The average signal and standard deviation ($\Delta\lambda_{SPR}$ ± SD) was graphed *versus* the injected analyte concentration. The data were fitted to a one-site specific binding model curve:

$$y = \frac{Ax}{B + x}$$

Where x is the concentration, y is the response signal, A is the extrapolated maximum signal obtained by the specific analyte and B is related to the equilibrium binding constant. The LOD (Limit of Detection) and the LOQ (Limit of Quantification) were calculated as the concentration corresponding to the blank signal plus three and ten times its SD respectively. BSA was used to confirm the specificity of the assays. Data analysis and fitting was performed using Origin Pro and GraphPad-Prism software.

Real sputum sample evaluation

For the evaluation of the sputum samples, non-tuberculous samples (UNTSS and PNTSS) as negative controls were tested. Undiluted UNTSS and PNTSS samples and PNTSS samples diluted 1:1 with PBST were injected in the biosensor at a flow rate of 30 μL min^{-1}. Each sample was measured by triplicate. In order to evaluate the accuracy of the assay, seven blind samples of known concentration of rHspX (B1-B6) were prepared in PNTSS using concentrations within and over the working range and then diluted in PBST 1:1 prior analysis. Blind samples B2, B4 and B6 with concentrations over the working range, required an additional dilution factor of 2, 3 and 5-fold respectively. The % Recovery was calculated as:

$$\text{Recovery } \% = \frac{[\mathbf{Blind\ sample}]_{calculated}}{[\mathbf{Blind\ sample}]_{real}} \times \mathbf{100}$$

Finally, 15 tuberculous samples PTSS (S1-S15) and 22 non-tuberculous samples PNTSS (S16-S37) were evaluated with the optimized protocol. Signals were interpolated in the calibration curve performed with PNTSS (1:1). Real samples were also measured in triplicate and the average, SD and the coefficient of variability (CV) were calculated.

Acknowledgements

The ICN2 is funded by the CERCA programme / Generalitat de Catalunya. The ICN2 is supported by the Severo Ochoa Centres of Excellence programme, funded by the Spanish Research Agency (AEI, grant no. SEV-2017-0706). We thank COLCIENCIAS for supporting this work through the grant No. 0375-2013 with number project 6570577636375 and the Universidad Central (Colombia) for supporting this work through the Research Cluster on Converging Sciences and Technology (NBIC). We also thank the clinician of La Paz University Hospital for helping in the recruitment of TB patients.

References

[1] Magana-Arachchi, D., Medagedara, D., Thevanesam, V. (2011) Molecular characterization of Mycobacterium tuberculosis isolates from Kandy, Sri Lanka. *Asian Pacific J. Trop. Dis.* 1, 181–186. doi:10.1016/S2222-1808(11)60024-8.

[2] Cheon, S.A., Cho, H.H., Kim, J., Lee, J., Kim, H.J., Park, T.J. (2016) Recent

tuberculosis diagnosis toward the end TB strategy. *J. Microbiol. Methods*. 123, 51–61. doi:10.1016/j.mimet.2016.02.007.

[3] World Health Organisation, Global Health TB Report, 2018.

[4] Goletti, D., Petruccioli, E., Joosten, S.A., Ottenhoff, T.H.M. (2016) Tuberculosis biomarkers: From diagnosis to protection. *Infect. Dis. Rep*. 8, 24–32. doi:10.4081/idr.2016.6568.

[5] Dheda, K., Barry, C.E., Maartens, G. (2016) Tuberculosis. *Lancet*. 387, 1211–1226. doi:10.1016/S0140-6736(15)00151-8.

[6] Wallis, R.S., Maeurer, M., Mwaba, P., Chakaya, J., Rustomjee, R.. Migliori, G.B., Marais, B., Schito, M., Churchyard, G., Swaminathan, S., Hoelscher, M., Zumla, A. (2016) Tuberculosis-advances in development of new drugs, treatment regimens, host-directed therapies, and biomarkers. *Lancet Infect. Dis.* 16, e34–e46. doi:10.1016/S1473-3099(16)00070-0.

[7] Marais, B.J. (2016) The global tuberculosis situation and the inexorable rise of drug-resistant disease. *Adv. Drug Deliv. Rev.* 102, 3–9. doi:10.1016/j.addr.2016.01.021.

[8] Yon Ju Ryu, M.D. (2015) Diagnosis of pulmonary tuberculosis: Recent advances and diagnostic algorithms. *Tuberc. Respir. Dis.* 78 (2), 64–71. doi:10.4046/trd.2015.78.2.64.

[9] Hong, S.C., Lee, J., Shin, H.C., Kim, C.M., Park, J.Y., Koh, K., Kim, H.J., Chang, C.L., Lee, J. (2011) Clinical immunosensing of tuberculosis CFP-10 in patient urine by surface plasmon resonance spectroscopy. *Sens. Act. B Chem.* 160, 1434–1438. doi:10.1016/j.snb.2011.10.006.

[10] Viñuelas-Bayón, J., Vitoria, M.A., Samper, S. (2017) Rapid diagnosis of tuberculosis. Detection of drug resistance mechanisms. *Enferm. Infecc. Microbiol. Clin.* 35, 520–528. doi:10.1016/j.eimc.2017.01.015.

[11] Bansal, R., Sharma, P.K., Jaryal, S.C., Gupta, P.K., Kumar, D. (2017) Comparison of Sensitivity and Specificity of ZN and Fluorescent Stain Microscopy with Culture as Gold Standard. *J. Tuberc. Res.* 5, 118–128. doi:10.4236/jtr.2017.52013.

[12] Reza, L.W., Satyanarayna, S., Enarson, D.A., Kumar, A.M.V., Sagili, K., Kumar, S., Prabhakar, L.A., Devendrappa, N.M., Pandey, A., Wilson, N., Chadha, S., Thapa, B., Sachdeva, K.S., Kohli, M.P. (2013) LED-Fluorescence Microscopy for Diagnosis of Pulmonary Tuberculosis under Programmatic Conditions in India. *PLoS One*. 8, e75566 doi:10.1371/journal.pone.0075566.

[13] Ismail, N.A., Omar, S. V., Lewis, J.J., Dowdy, D.W., Dreyer, A.W., Van Der Meulen, H., Nconjana, G., Clark, D.A., Churchyard, G.J. (2015) Performance of a novel algorithm using automated digital microscopy for diagnosing tuberculosis. *Am. J. Respir. Crit. Care Med.* 191, 1443–1449. doi:10.1164/rccm.201502-0390OC.

[14] Ruhwald, M., Aggerbeck, H. , Gallardo, R.V., Hoff, S.T., Villate, J.I., Borregaard, B.,

Martinez, J.A., Kromann, I., Penas, A., Anibarro, L.L., de Souza-Galvão, M.L., Sánchez, F., Rodrigo-Pendás, J.Á., Noguera-Julian, A., Martínez-Lacasa, X., Tuñez, M.V., Fernández, V.L., Millet, J.P., Moreno, A., Cobos, N., Miró, J.M., Roldan, L., Orcau, A., Andersen, P., Caylá, J.A. (2017) Safety and efficacy of the C-Tb skin test to diagnose Mycobacterium tuberculosis infection, compared with an interferon γ release assay and the tuberculin skin test: a phase 3, double-blind, randomised, controlled trial. *Lancet Respir. Med.* 5, 259–268. doi:10.1016/S2213-2600(16)30436-2.

[15] Mazurek, G.H., Jereb, J., Vernon, A., LoBue, P., Goldberg, S., Castro, K. (2010) Updated guidelines for using interferon gamma release assays to detect Mycobacterium tuberculosis infection-United States. *Morb. Mortal. Wkly Rep.* 59, 1–25. doi:10.1097/00043764-197203000-00020.

[16] Ling, D.I., Nicol, M.P., Pai, M., Pienaar, S., Dendukuri, N., Zar, H.J. (2013) Incremental value of T-SPOT.TB for diagnosis of active pulmonary tuberculosis in children in a high-burden setting: A multivariable analysis. *Thorax*. 68, 860–866. doi:10.1136/thoraxjnl-2012-203086.

[17] Mori, Y., Kanda, H., Notomi, T. (2013) Loop-mediated isothermal amplification (LAMP): Recent progress in research and development. *J. Infect. Chemother.* 19, 404–411. doi:10.1007/s10156-013-0590-0.

[18] Nagai, K., Horita, N., Yamamoto, M., Tsukahara, T., Nagakura, H., Tashiro, K., Shibata, Y., Watanabe, H., Nakashima, K., Ushio, R., Ikeda, M., Narita, A., Kanai, A., Sato, T., Kaneko, T. (2016) Diagnostic test accuracy of loop-mediated isothermal amplification assay for Mycobacterium tuberculosis: Systematic review and meta-analysis. *Sci. Rep.* 6, 3–9. doi:10.1038/srep39090.

[19] Chakravorty, S., Simmons, A.M., Rowneki, M., Parmar, H., Cao, Y., Ryan, J., Banada, P.P., Deshpande, S., Shenai, S., Gall, A., Glass, J., Krieswirth, B., Schumacher, S.G., Nabeta, P., Tukvadze, N., Rodrigues, C., Skrahina, A., Tagliani, E., Cirillo, D.M., Davidow, A., Denkinger, C.M., Persing, D., Kwiatkowski, R., Jones, M., Alland, D. (2017) The New Xpert MTB/RIF Ultra: Improving Detection of Mycobacterium tuberculosis and Resistance to Rifampin in an Assay Suitable for Point-of-Care Testing. *MBio.* 8, 1–12. doi:10.1128/mbio.00812-17.

[20] Ramirez-Priego, P., Martens, D., Elamin, A.A., Soetaert, P., Van Roy, W., Vos, R., Anton, B., Bockstaele, R., Becker, H., Singh, M., Bienstman, P., Lechuga, L.M. (2018) Label-Free and Real-Time Detection of Tuberculosis in Human Urine Samples Using a Nanophotonic Point-of-Care Platform. *ACS Sensors.* 3, 2079–2086. doi:10.1021/acssensors.8b00393.

[21] Mukundan, H., Kumar, S., Price, D.N., Ray, S.M., Lee, Y.J., Min, S., Eum, S., Kubicek-Sutherland, J., Resnick, J.M., Grace, W.K., Anderson, A.S., Hwang, S.H., Cho, S.N.,

Via, L.E., Barry, C., Sakamuri, R., Swanson, B.I. (2012) Rapid detection of Mycobacterium tuberculosis biomarkers in a sandwich immunoassay format using a waveguide-based optical biosensor. *Tuberculosis.* 92, 407–416. doi:10.1016/j.tube.2012.05.009.

[22] Poulakis, N., Gritzapis, A.D., Ploussi, M., Leventopoulos, M., Papageorgiou, C. V., Anastasopoulos, A., Constantoulakis, P., Karabela, S., Vogiatzakis, E., Tsilivakos, V. (2016) Intracellular ESAT-6: A new biomarker for Mycobacterium tuberculosis infection. *Cytom. Part B - Clin. Cytom.* 90, 312–314. doi:10.1002/cyto.b.21220.

[23] Ren, N., JinLi, J., Chen, Y., Zhou, X., Wang, J., Ge, P., Khan, F.A., Zhang, L., Hu, C., Robertson, I.D., Chen, H., Guo, A. (2018) Identification of new diagnostic biomarkers for Mycobacterium tuberculosis and the potential application in the serodiagnosis of human tuberculosis. *Microb. Biotechnol*. 11, 893–904. doi:10.1111/1751-7915.13291.

[24] Haldar, S., Sankhyan, N., Sharma, N., Bansal, A., Jain, V., Gupta, V.K., Juneja, M., Mishra, D., Kapil, A., Singh, U.B., Gulati, S., Kalra, V., Tyagi, J.S. (2012) Detection of Mycobacterium tuberculosis GlcB or HspX Antigens or devR DNA Impacts the Rapid Diagnosis of Tuberculous Meningitis in Children. *PLoS One.* 7, e0044630. doi:10.1371/journal.pone.0044630.

[25] de Sousa, E.M., da Costa, A.C., Trentini, M.M., de Araújo Filho, J.A., Kipnis, A., Junqueira-Kipnis, A.P. (2012) Immunogenicity of a Fusion Protein Containing Immunodominant Epitopes of Ag85C, MPT51, and HspX from Mycobacterium tuberculosis in Mice and Active TB Infection *PLoS One.* 7, e0047781 doi:10.1371/journal.pone.0047781.

[26] Rajpal, S.K., Snehal, S.W., Milind, S.P., Hemant, J.P., Girdhar, M.T., Hatim, F.D. (2011) Mycobacterium Tuberculosis Heat Shock Protein 16 as a Potential Marker for Latent TB: A Preliminary Findings. *J. Clin. Cell. Immunol.* 2, 115 doi:10.4172/2155-9899.1000115.

[27] Shekhawat, S.D., Jain, R.K., Gaherwar, H.M., Purohit, H.J., Taori, G.M., Daginawala, H.F., Kashyap, R.S. (2014) Heat shock proteins: Possible biomarkers in pulmonary and extrapulmonary tuberculosis. *Hum. Immunol.* 75, 151–158. doi:10.1016/j.humimm.2013.11.007.

[28] Wu, X., Yang, Y., Zhang, J., Li, B., Liang, Y., Zhang, C., Dong, M. (2010) Comparison of antibody responses to seventeen antigens from Mycobacterium tuberculosis. *Clin. Chim. Acta*. 411, 1520–1528. doi:10.1016/j.cca.2010.06.014.

[29] Pai, M., Behr, M., Dowdy, D., Dheda, K., Divangahi, M., Boehme, C., Ginsberg, A., Swaminathan, S., Spigelman, M., Getahun, H., Menzies, D., Raviglione, M. (2016) Tuberculosis. *Lancet.* 2, 1–23. doi:10.1016/S0140-6736(19)30308-3.

[30] Srivastava, S.K., van Rijn, C.J.M., Jongsma, M.A. (2016) Biosensor-based detection of

tuberculosis. *RSC Adv.* 6, 17759–17771. doi:10.1039/C5RA15269K.

[31] Shah, M, Hanrahan, C, Wang, ZY, Dendukuri, N, Lawn, SD, Denkinger, CM, Steingart, KR. (2016) Lateral flow urine lipoarabinomannan assay for detecting active tuberculosis in HIV-positive adults. Cochrane Database of Systematic Reviews, 5, CD011420 10.1002/14651858.CD011420.pub2

[32] Zou, F., Wang, X., Qi, F., Koh, K., Lee, J., Zhou, H., Chen, H. (2017) Magneto-plamonic nanoparticles enhanced surface plasmon resonance TB sensor based on recombinant gold binding antibody. *Sens. Act. B Chem.* 250, 356–363. doi:10.1016/j.snb.2017.04.162.

[33] Hong, S.C., Chen, H., Lee, JPark, ., H.-K., Kim, Y.S., Shin, H.-C., Kim, C.-M., Park, T.J., Lee, S.J., Koh, K., Kim, H.-J., Chang, C.L., Lee, J. (2011) Ultrasensitive immunosensing of tuberculosis CFP-10 based on SPR spectroscopy. *Sens. Act. B Chem.* 156, 271–275. doi:10.1016/j.snb.2011.04.032.

[34] Trzaskowski, M., Napiórkowska, A., Augustynowicz-Kopeć, E., Ciach, T. (2018) Detection of tuberculosis in patients with the use of portable SPR device. *Sens. Act. B Chem.* 260, 786–792. doi:10.1016/j.snb.2017.12.183.

[35] Shabut, A.M., Hoque Tania, M., Lwin, K.T., Evans, B.A., Yusof, N.A., Abu-Hassan, K.J., Hossain, M.A. (2018) An intelligent mobile-enabled expert system for tuberculosis disease diagnosis in real time. *Expert Syst. Appl.* 114, 65–77. doi:10.1016/j.eswa.2018.07.014.

[36] Bhattacharyya, D., Smith, Y.R., Mohanty, S.K., Misra, M. (2016) Titania Nanotube Array Sensor for Electrochemical Detection of Four Predominate Tuberculosis Volatile Biomarkers. *J. Electrochem. Soc.* 163, B206–B214. doi:10.1149/2.0221606jes.

[37] Hsieh, S.C., Chang, C.C., Lu, C.C., Wei, C.F., Lin, C.S., Lai, H.C., Lin, C.W. (2012) Rapid identification of Mycobacterium tuberculosis infection by a new array format-based surface plasmon resonance method. *Nanoscale Res. Lett.* 7, 1–6. doi:10.1186/1556-276X-7-180.

[38] Thanyani, S.T., Roberts, V., Siko, D.G.R., Vrey, P., Verschoor, J. A. (2008) A novel application of affinity biosensor technology to detect antibodies to mycolic acid in tuberculosis patients. *J. Immunol. Methods.* 332, 61–72. doi:10.1016/j.jim.2007.12.009.

[39] Steingart, K.R., Henry, M., Laal, S., Hopewell, P.C., Ramsay, A., Menzies, D., Cunningham, J., Weldingh, K., Pai, M. (2007) Commercial serological antibody detection tests for the diagnosis of pulmonary tuberculosis: A systematic review. *PLoS Med.* 4, 1041–1060. doi:10.1371/journal.pmed.0040202.

[40] Wallis, R.S., Pai, M., Menzies, D., Doherty, T.M., Walzl, G., Perkins, M.D., Zumla, A. (2010) Biomarkers and diagnostics for tuberculosis: progress, needs, and translation into practice. *Lancet.* 375, 1920–1937. doi:10.1016/S0140-6736(10)60359-5.

[41] Castro-Garza, J., García-Jacobo, P., Rivera-Morales, L.G., Quinn, F.D., Barber, J., Karls, R., Haas, D., Helms, S., Gupta, T., Blumberg, H., Tapia, J., Luna-Cruz, I., Rendon, A., Vargas-Villarreal, J., Vera-Cabrera, L., Rodríguez-Padilla, C. (2017) Detection of anti-HspX antibodies and HspX protein in patient sera for the identification of recent latent infection by Mycobacterium tuberculosis. *PLoS One.* 12, e0181714. doi:10.1371/journal.pone.0181714.

[42] Yousefi-Avarvand, A., Tafaghodi, M., Soleimanpour, S., Khademi, F. (2018) HspX protein as a candidate vaccine against Mycobacterium tuberculosis: an overview. *Front. Biol.* 13, 293–296. doi:10.1007/s11515-018-1494-2.

[43] Taylor, J.L., Wieczorek, A., Keyser, A.R., Grover, A., Flinkstrom, R., Karls, R.K., Bielefeldt-Ohmann, H., Dobos, K.M., Izzo, A.A. (2012) HspX-mediated protection against tuberculosis depends on its chaperoning of a mycobacterial molecule. *Immunol. Cell Biol*. 90, 945-954. doi:10.1038/icb.2012.34.

[44] Kennaway, C.K., Benesch, J.L.P., Gohlke, U., Wang, L., Robinson, C. V., Orlova, E. V., Saibi, H.R., Keep, N.H. (2005) Dodecameric structure of the small heat shock protein Acr1 from Mycobacterium tuberculosis. *J. Biol. Chem.* 280, 33419–33425. doi:10.1074/jbc.M504263200.

[45] Kaushik, A., Singh, U.B., Porwal, C., Venugopal, S.J., Mohan, A., Krishnan, A., Goyal, V., Banavaliker, J.N. (2012) Diagnostic potential of 16 kDa (HspX, alpha-crystalline) antigen for serodiagnosis of tuberculosis. *Indian J. Med. Res.* 135, 771–777.

[46] Zhang, C., Song, X., Zhao, Y., Zhang, H., Zhao, S., Mao, F., Bai, B., Wu, S., Shi, C. (2015) Mycobacterium tuberculosis Secreted Proteins As Potential Biomarkers for the Diagnosis of Active Tuberculosis and Latent Tuberculosis Infection. *J. Clin. Lab. Anal.* 29, 375–382. doi:10.1002/jcla.21782.

[47] Limongi, A., Olival, L., Conde, M.B., Junqueira-Kipnis, A.P. (2011) Determination of levels of specific IgA to the HspX recombinant antigen of Mycobacterium tuberculosis for the diagnosis of pleural tuberculosis. *J Bras Pneumol.* 37, 302–307.

[48] Rabahi, M.F., Junqueira-Kipnis, A.P., dos Reis, M.C.G., Oelemann, W., Conde, M.B. (2007) Humoral response to HspX and GlcB to previous and recent infection by Mycobacterium tuberculosis. *BMC Infect. Dis.* 7, 1–9. doi:10.1186/1471-2334-7-148.

[49] Fu, X., Zhang, H., Zhang, X., Cao, Y., Jiao, W., Liu, C., Song, Y., Abulimiti, A., Chang, Z. (2005) A dual role for the N-terminal region of Mycobacterium tuberculosis Hsp16.3 in self-oligomerization and binding denaturing substrate proteins. *J. Biol. Chem.* 280, 6337–6348. doi:10.1074/jbc.M406319200.

[50] De Vos, K., Girones, J., Popelka, S., Schacht, E., Baets, R., Bienstman, P. (2009) SOI optical microring resonator with poly(ethylene glycol) polymer brush for label-free biosensor applications. *Biosens. Bioelectron.* 24, 2528–2533.

doi:10.1016/j.bios.2009.01.009.

[51] Holz, O., Kips, J., Magnussen, H. (2000) Update on sputum methodology. *Eur. Respir. J.* 16, 355–359. doi:10.1034/j.1399-3003.2000.16b26.x.

[52] Cubero, N., Esteban, J., Palenque, E., Rosell, A., Garcia, M.J. (2013) Evaluation of the detection of Mycobacterium tuberculosis with metabolic activity in culture-negative human clinical samples. *Clin. Microbiol. Infect.* 19, 273–278. doi:10.1111/j.1469-0691.2012.03779.x.

[53] Bannantine, J.P., Stabel, J.R. (2000) HspX is present within Mycobacterium paratuberculosis-infected macrophages and is recognized by sera from some infected cattle. *Vet. Microbiol.* 76, 343–58. http://www.ncbi.nlm.nih.gov/pubmed/11000531.

[54] Soler, M., Estevez, M.C., Moreno, M.L., Cebolla, A., Lechuga, L.M. (2016) Label-free SPR detection of gluten peptides in urine for non-invasive celiac disease follow-up. *Biosens. Bioelectron.* 79, 158–164. doi:10.1016/j.bios.2015.11.097.

FOR TABLE OF CONTENTS ONLY